




# Non-invasive and wearable glucose biosensor based on gel electrolyte for detection of human sweat

Nan Gao<sup>1</sup>, Zhiwei Cai<sup>1</sup>, Gang Chang<sup>1,\*</sup> , and Yunbin He<sup>1,\*</sup>

<sup>1</sup> Ministry-of-Education Key Laboratory for the Green Preparation and Application of Functional Materials, Hubei Key Laboratory of Polymer Materials, School of Materials Science and Engineering, Hubei University, No.368 Youyi Avenue, Wuchang, Wuhan 430062, China

**Received:** 13 September 2022

**Accepted:** 15 December 2022

**Published online:**

3 January 2023

© The Author(s), under exclusive licence to Springer Science+Business Media, LLC, part of Springer Nature 2023

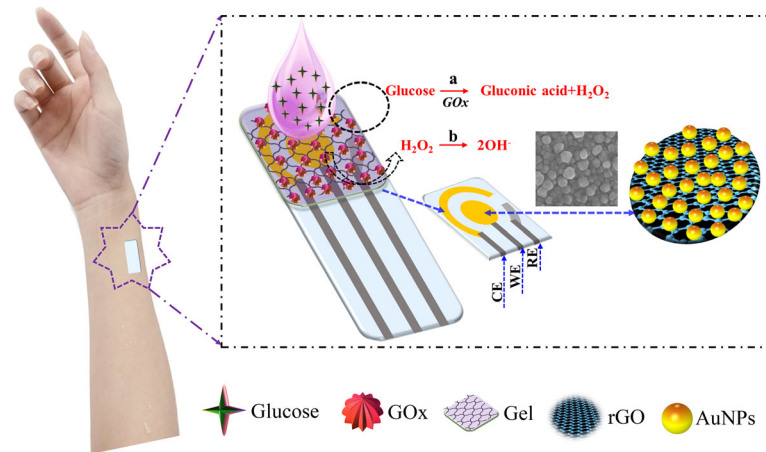
## ABSTRACT

Flexible, wearable biosensors have been extensively investigated in recent decades due to their potential applications in portable electronics and human health monitoring. However, low sensitivity and complex fabrication are still great challenges for flexible sensors. Herein, a flexible electrochemical biosensor for glucose was proposed, which was based on reduced graphene oxide and gold nanoparticle-modified screen-printed gold electrodes (rGO-Au/SPGE) as catalysts and gel instead of traditional liquid electrolyte. The biosensor combines the soft stretchability of the gel, the specific selectivity of glucose oxidase (GOx) and the high catalytic activity of the rGO-Au/SPGE nanocomposite. More importantly, the soft gel not only adheres well to the skin, but also promotes the penetration of water-soluble molecules, effectively improving the accumulation of bodily fluids on dry skin surfaces. The constructed GOx-gel-rGO-Au/SPGE biosensor maintains stable sensing performance even after 1000 bending cycles. In addition, the biosensor exhibited significantly current response to glucose at a detection range of 1.25–850  $\mu\text{M}$  and 0.85–7.72 mM (covers the glucose level in human sweat), with a sensitivity of 53.7 and 27.4  $\mu\text{A}/\text{mM cm}^2$  and low detection limit (1.25  $\mu\text{M}$ ). The flexible electrochemical biosensor based on GOx-gel-rGO-Au/SPGE could accurately determine glucose in human sweat, demonstrating a promising feature for personal healthcare diagnosis.

Handling Editor: Annela M. Seddon.

Address correspondence to E-mail: gchanghubei@gmail.com; ybhe@hubu.edu.cn

## GRAPHICAL ABSTRACT



## Introduction

Flexible and wearable technology is one of the rapidly developing industries in recent years. It is widely used in human physiological activity monitoring, disease prevention, artificial skin and human-computer interaction fields [1–3]. In particular, with the growing awareness of health care, the medical wearable market has promoted from the current hospital-centered treatment to patient-centered diagnosis [4, 5]. Glucose sensor has important application value in physicochemical sensors related to health and medical care [6, 7]. Diabetes is a common disease that endangers people's health. Patients need to be regularly monitored for blood glucose in order to receive timely and correct treatment [6, 8]. The traditional fingertip blood collection method often brings physical pain and psychological pressure for patients. It is particularly urgent to develop a non-invasive and wearable glucose sensor. As an innate body fluid, human sweat contains various physiological markers, which could realize the non-invasive measurement of human glucose level [9, 10]. Meanwhile, people with diabetes or metabolic abnormalities have higher-than-normal levels of glucose in their sweat [11]. Studies have confirmed that there is a certain relationship between the

glucose content in sweat and human blood sugar levels [12, 13]. Therefore, the development of an in situ non-invasive glucose sensor for monitoring sweat has important practical significance for real-time evaluation of human health and clinical diagnosis. Due to the complex chemical environment of human sweat, the high selectivity of the sensor is crucial. Glucose oxidase (GOx) has high selectivity and sensitivity, and enzymatic glucose biosensors are considered to be the ideal choice for wearable sensors.

Conventional flexible substrates of non-invasive wearable biosensors are currently dominated by polyethylene terephthalate (PET) [14] or polyimide (PI) [15, 16]. However, due to the mismatch between the sensor substrate and the epidermis would lead to sweat accumulation and inaccurate detection. An ideal wearable sensor is required to maintain excellent performance when subjected to severe deformation such as bending, stretching and even twisting. In addition, they need to be biocompatible and non-toxic to ensure that they do not damage clothing or skin, and could function in moist bodily fluids. Hydrogels consist of polymer network structures containing more than 90% water and could be ideal ionic conductors [17]. Compared with traditional conductive materials, hydrogels have good swelling properties and biocompatibility [17, 18]. The

hydrogel is able to adapt to the dynamic properties of the skin, creating a good contact between the sensors and human skin even under severe deformation. The unique three-dimensional network structure of hydrogels is more conducive to the diffusion and collection of small molecules, which effectively solves the problem of body fluid collection of wearable sensors [19, 20]. Solid gel replaces traditional liquid electrolyte, providing a favorable platform for real-time monitoring of non-invasive wearable sensors. In addition, glycerol is often introduced to solve the problem of water absorption and shrinkage of hydrogels.

Recently, nanomaterials with high surface area, high conductivity and electrochemical activity have attracted growing attention in the sensing field. In order to effectively improve the sensitivity of sensors, reduced graphene oxide (rGO) is often used as a supporting substrate for nanomaterials [21, 22]. For instance, the Ag-CuO/rGO nanocomposite was constructed as a novel non-enzymatic glucose sensor, with the synergistic effect of Ag, CuO and rGO, the sensor exhibited excellent catalytic performance for glucose detection [23]. Liu and co-workers [24] combined porous enzyme nanofiber membranes with PtNPs/graphene nanocomposites to facilitate electron transport between enzymes and electrodes, thereby improving the catalytic performance of glucose and lactate. Over the past few decades, Au nanomaterials-based electrodes frequently appear in various types of stretchable biological analysis fields, indicating that they have broad prospects in wearable electrochemical biosensors [25, 26].

Herein, a flexible and wearable glucose electrochemical biosensor based on reduced graphene oxide/gold nanoparticle-modified screen-printed gold electrodes (rGO-Au/SPGE) and hydrogel as electrolyte was fabricated. The controllable and in situ formation of rGO-Au nanocomposites onto SPGE was achieved via a one-step electrodeposition strategy. And the porous gel was synthesized by polymerization reaction to replace the liquid electrolyte, thus achieving moisturization and GOx fixation and effect. The feasibility and electrochemical properties of the gel as electrolyte were characterized using electrochemical methods. The mechanical stability and sensing performance of the constructed biosensor were verified by bending cycle experiments. In addition, the detection results of the constructed sensor in human sweat were compared with

commercial enzyme kits to evaluate the accuracy of the sensor in practical application.

## Experimental

### Reagents and instruments

Single-layer graphene oxide (GO) was purchased from XFNANO (Nanjing, China). Glucose oxidase (GOx, 100 U mg<sup>-1</sup>), chloroauric acid trihydrate (HAuCl<sub>4</sub>·3H<sub>2</sub>O), ammonium persulphate, acrylamide and N, N, N', N'-tetramethylethylenediamine were procured from Aldrich Co., Ltd. Ethanol, NaCl, KCl, Na<sub>2</sub>HPO<sub>4</sub>·12H<sub>2</sub>O, NaH<sub>2</sub>PO<sub>4</sub>·2H<sub>2</sub>O, D(+) -glucose monohydrate, glycerol and chitosan (white mushroom, high molecular weight), and N, N'-methylene diacrylamide were all obtained from Sinopharm Chemical Reagent. Dopamine (DA), uric acid (UA), ascorbic acid (AA), lactic acid and urea were purchased from Shanghai Macklin Biochemical Co., Ltd. Nafion (5 wt% in low aliphatic alcohols) was supplied by Du Pont. Phosphate-buffered saline (PBS) was prepared with NaH<sub>2</sub>PO<sub>4</sub>·2H<sub>2</sub>O and Na<sub>2</sub>HPO<sub>4</sub>·12H<sub>2</sub>O. D(+) glucose solution was diluted in 0.1 M phosphate-buffered saline (PBS, pH 7.4) and allowed to stand for 24 h prior to use to allow equilibration. Deionized water was obtained from the water purification system P60-CY (Kertone Water Treatment Co., Ltd). During the experiment, deionized water was used for all reagent dissolution and glassware cleaning.

Screen printing gold electrode (SPGE) was produced by Qingdao Poten Technology Co., Ltd., the working electrode ( $D = 4$  mm) and the counter electrode were made of gold electrodes, the Ag/AgCl electrode prepared by silver ink was used as the reference electrode, and polyimide (PI) was used as the flexible substrate. Cyclic voltammetry (CV) and chronoamperometry ( $i-t$ ) were carried out on a CHI660e electrochemical workstation (CH, Shanghai, China). The morphology of the working electrode and the thickness of the prepared gel were characterized by field emission scanning electron microscopy (FE-SEM, ZEISS, Germany) with energy-dispersive X-ray spectroscopy (EDX). The crystal structure of the prepared material was determined by X-ray diffractometer (XRD, D8A25, BRUKER Technology Co., Ltd., USA). The resistivity of the prepared gel was measured using 4-point probe

resistivity measurement system (RTS-9, Guangzhou, China). UV 3600 Plus (Shimadzu Corporation, Japan) was used to test the absorbance of glucose. Additionally, all the experimental measurements were carried out at normal temperature.

### Synthesis of rGO-Au/SPGE

The single-layer GO was dissolved in deionized water and dispersed by ultrasonic to form a uniform solution of  $0.5 \text{ mg mL}^{-1}$ .  $25 \text{ }\mu\text{L}$  graphene dispersed droplets were placed on the surface of SPGE working electrode, fixed with Nafion and dried at room temperature. rGO-Au/SPGE was synthesized by CV scanning 6 cycles from 0.0 to  $-1.5 \text{ V}$  in  $1.0 \text{ mM}$   $\text{HAuCl}_4$  solution. Finally, the electrode was gently rinsed with deionized water and stored in the refrigerator for use in the next step. As a comparison, rGO/SPGE and Au/SPGE were prepared in the same method.

### Preparation of gel electrolyte

Using a simple polymerization reaction, the two solutions labeled A and B are mixed to synthesize gel electrolyte [12, 27]. In the preparation process, acrylamide was used as monomer, N, N'-methylene diacrylamide as crosslinking agent, N, N, N', N'-tetramethylethylenediamine as accelerator and ammonium persulfate as initiator.  $0.6 \text{ M}$  NaCl and glycerol were used as solvents ( $V/V = 5:1$ ) to ensure the preparation of hydrogel with good electrical conductivity and water retention. Dissolve  $0.4 \text{ g}$  acrylamide,  $0.015 \text{ g}$  N, N'-methylene diacrylamide and  $30 \text{ }\mu\text{L}$  N, N, N', N'-tetramethylethylenediamine in  $6 \text{ mL}$  solvent to prepare solution A. Similarly, solution B was composed of  $4 \text{ g}$  ammonium persulfate dissolved in  $12 \text{ mL}$  of solvent. Solutions A and B ( $V/V = 1:2$ ) were mixed in an ice bath environment, and the mixture was coated on a clean glass surface and quickly covered by another piece of glass. The film could be formed after about  $10 \text{ s}$ . In order to enhance the moisture retention of the gel, the prepared gel was peeled off and soaked in glycerin for overnight storage. Finally, the gel was taken out to dry and cut into sizes of  $1.1 \text{ cm} \times 1.2 \text{ cm}$ .  $5 \text{ }\mu\text{L}$   $5 \text{ mg mL}^{-1}$  GOx was dropped onto the surface of gel, then dripped chitosan solution on the surface to achieve stable anchoring of the coating and placed at  $4 \text{ }^\circ\text{C}$  to dry overnight before use.

### Fabrication of the biosensor

The fabrication process of glucose biosensor was depicted in Scheme 1. First, the gel was carefully transferred to the surface of the rGO-Au/SPGE. During the transfer, it is necessary to make sure that the gel was in close contact with the electrode and no bubbles existed; otherwise, the stability of the electrode would be affected.  $3 \text{ }\mu\text{L}$  glucose standard solution of different concentrations was dropped onto the gel surface, and data were collected by *i-t* method. The detection mechanism was as follows: Under the action of GOx, glucose was decomposed on the surface of the gel into glucose acid and hydrogen peroxide ( $\text{H}_2\text{O}_2$ ) (Reaction a). After that, the small molecules of  $\text{H}_2\text{O}_2$  pass through the gel and contact the rGO-Au catalyst, and the reduction reaction occurs to generate hydroxide ( $\text{OH}^-$ ), thereby generating the response current (Reaction b).

### Human sweat samples handle and measurement procedure

Fresh sweat from two volunteers was collected as practical samples. About  $3 \text{ mL}$  of sweat was collected on the surface of the volunteers' arms after playing badminton.  $5 \text{ }\mu\text{L}$  sweat samples were dropped onto the surface of GOx-gel-rGO-Au/SPGE to record the current response of *i-t*. As a control, a commercial glucose enzyme kit was used to test sweat samples to verify the accuracy of the prepared biosensor. To truly reflect that the constructed sensor could be worn on the human body to achieve the purpose of real-time monitoring, during the attachment experiment, the sensor was directly attached to the human skin surface.

### Ethics statement

All experiments were conducted in accordance with the relevant laws and institutional guidelines from the Zijing Hospital (Wuhan, China) and "Regulations on the Administration of Medical Institutions" from China and were approved by the Ethics Committee of Hubei University. All experiments were performed in compliance with the laws of the People's Republic of China. Informed consents were obtained from all volunteers for this experiment.



**Scheme 1** Schematic illustration of the construction of a glucose biosensor and its sensing principle in sweat.

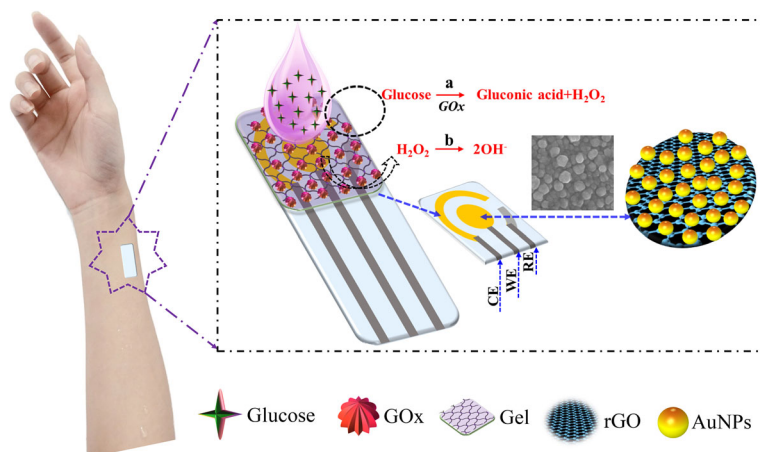
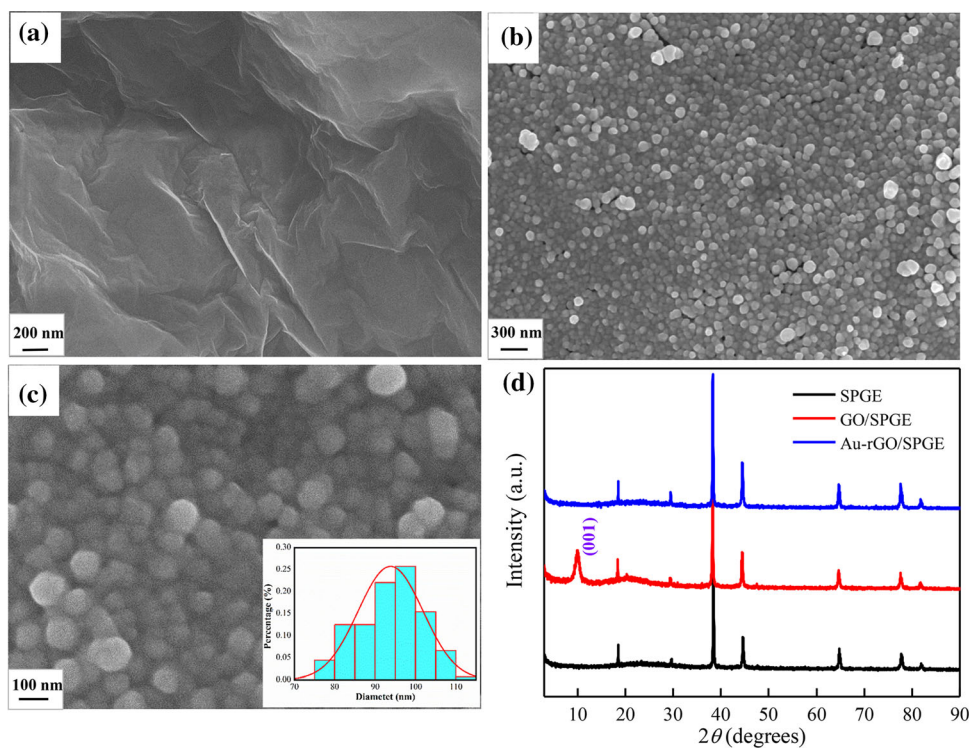


**Figure 1** FE-SEM images of GO (a), Au-rGO nanocomposite (b) and Au-rGO nanocomposite at high magnification (c). The particle size distribution of AuNPs (inset of c); (d) the XRD pattern of SPGE, GO/SPGE and Au-rGO/SPGE nanocomposite..



## Results and discussion

### Characterization of the synthesis nanomaterials

The prepared rGO was characterized by FE-SEM. As shown in Fig. 1a, the rGO film exhibited a typical light yarn fold-like structure layer, which could effectively increase the surface area of the working electrode. In Fig. 1b and c, AuNPs were reduced on the surface of rGO film, and spherical AuNPs with the size of about 100 nm were evenly distributed on the wrinkled rGO without agglomeration. In

addition, Fig. S1 shows the corresponding element mapping distribution of the prepared material. Au, C and O elements were uniformly distributed on the surface of rGO-Au nanocomposites, which confirmed the existence of AuNPs and rGO. All these results demonstrated that the rGO-Au nanocomposite could be successfully synthesized by electrodeposition. One of the highlights of our work is to replace traditional liquid electrolytes with gels for flexible, wearable biosensor monitoring. In Fig. S2, it was observed that the thickness of the gel was uniform at approximately 160  $\mu\text{m}$ . A typical four-probe system was used to

determine the gel resistivity of 1736.5  $\Omega$  cm, and the relative standard deviation (RSD) was 3.4% ( $n = 5$ ). The results show that the gel has uniform thickness and good conductivity, which provides a favorable guarantee for its use as a solid electrolyte.

The crystal structure and purity of the rGO-Au nanocomposite were further determined by XRD. As shown in Fig. 1d, there were obvious Au characteristic diffraction peaks on the bare electrode with sharp peaks, indicating that SPGE as the substrate has good crystallinity and conductivity. The typical diffraction peaks corresponding to monolayer GO (001) were clearly observed on the electrode surface before electrodeposition. After electrodeposition in HAuCl<sub>4</sub> solution, it was observed that the diffraction peak of GO disappeared, while the diffraction peak of metallic gold tended to increase. This indicated that the deposition process could simultaneously reduce GO and Au<sup>3+</sup>, which was consistent with the above FE-SEM analysis.

### Electrochemical behaviors of the electrode materials

Using [Fe(CN)<sub>6</sub>]<sup>3-/4-</sup> as probe, the electron transfer behavior of different modified electrodes was investigated in 0.1 M KCl solution containing 5 mM [Fe(CN)<sub>6</sub>]<sup>3-/4-</sup> (Fig. 2a). GOx-gel/SPGE (curve a), GOx-gel-Au/SPGE (curve b), GOx-gel-rGO/SPGE (curve c) and GOx-gel-rGO-Au/SPGE (curve d) all showed a pair of obvious redox peaks. The oxidation peak potential was about 0.13 V, and the reduction peak potential was about -0.04 V. This was a typical Fe<sup>2+</sup>/Fe<sup>3+</sup> redox peaks peak pair, which visually

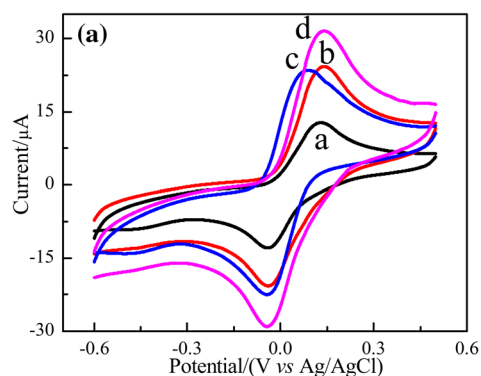


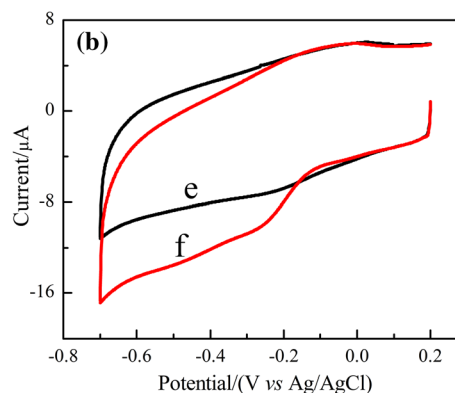
**Figure 2** (a) CV curves of GOx-gel/SPGE (curve a), GOx-gel-Au/SPGE (curve b), GOx-gel-rGO/SPGE (curve c) and GOx-gel-rGO-Au/SPGE (curve d) in 5.0 mM Fe(CN)<sub>6</sub><sup>3-/4-</sup> solution

demonstrated that small molecules could be contacted with the catalyst on the electrode surface through the gel and react chemically. On the other hand, under the synergistic effect of the large specific surface area of rGO and the high catalytic activity of AuNPs, the current response value of curve d was the largest, indicating that GOx-gel-rGO-Au/SPGE has the fastest electron transfer rate in the electrocatalytic process.

To explore the glucose detection mechanism of the constructed biosensor, CV images of GOx-gel-rGO-Au/SPGE in 0.1 M PBS solution without and with 1.2 mM glucose were investigated. In Fig. 2b, no significant peak was observed in the CV curve (curve e) of GOx-gel-rGO-Au/SPGE in 0.1 M PBS solution. After glucose was added, a significant reduction peak appeared on curve f around -0.1 V. This corresponds to the reduction process of hydrogen peroxide (a by-product of glucose under the action of GOx). The electrocatalytic properties of different modified electrodes for glucose were analyzed by *i-t* method. As shown in Fig. S3, under the synergistic action of rGO and AuNPs, GOx-gel-rGO-Au/SPGE (curve d) has excellent electrocatalytic performance for glucose. The above phenomenon was basically consistent with the analysis result of Fig. 2a.

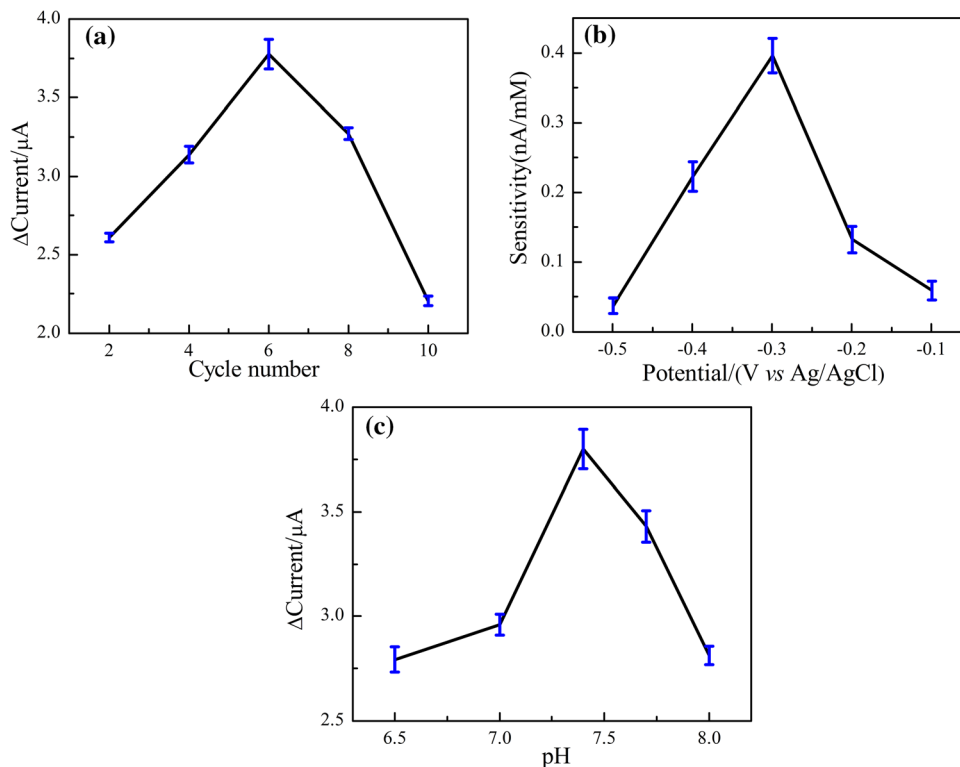
### Optimize the number of deposition cycles, working potential and pH value

In order to obtain the best detection performance of the glucose biosensor, the number of deposition cycles, the working potential and the pH value of the electrolyte were systematically optimized.



containing 0.1 M KCl. Scan rate: 50 mV s<sup>-1</sup>. (b) CV curves of GOx-gel-rGO-Au/SPGE without (e) and with 1.2 mM glucose (f) in 0.1 M PBS solution, scanning rate: 50 mV s<sup>-1</sup>.

**Figure 3** (a) The number of electrodeposition cycles, (b) the working potential and (c) the influence of pH value of electrolyte on glucose detection.



AuNPs have good catalytic activity, and its load quality is crucial to the sensitivity of glucose biosensors. In Fig. 3a, the current response of the biosensor to glucose gradually increases with the increase of the deposition cycles. When the number of deposition cycles reaches 6, the current response of the biosensor reaches the maximum value. This was attributed to the excessive amount of AuNPs generated which would cause agglomeration of particles and reduce the active sites, resulting in a decrease in the sensitivity of the biosensor. In addition, the deposition cycle number also affects the electrochemical activity of rGO. rGO has excellent electron transmission performance. However, excessive deposition cycles would lead to the stacking of rGO and decrease the electron mobility, weakening the electrochemical activity of rGO. Therefore, the electrodeposition cycle number 6 was selected for further investigations.

To get the highest sensitivity in the sensor performance analysis, it is crucial to use the appropriate working potential. Figure 3b shows the sensitivity of GOx-gel-rGO-Au/SPGE with a continuous addition of glucose at different potentials (from  $-0.1$  to  $-0.5$  V). It could be observed that when the working potential was  $-0.3$  V, the current of the biosensor

changes greatly and the response sensitivity was high. What's more, that low working potential could effectively reduce the interference signals from other electroactive substances in the real sample environment.

The pH value of electrolyte plays an important role in enzyme activity and biosensor stability. Figure 3c shows the current response of the glucose biosensor in the pH range of 6.5–8.0. And the maximum current response was obtained at pH 7.4. Too acidic or too alkaline an environment could seriously affect the activity of GOx. Based on this result, pH 7.4 was selected as the optimum electrolyte pH for the subsequent experiments.

### Analytical performance of the glucose biosensor

Under the optimized conditions, the glucose-sensing performance of the GOx-gel-rGO-Au/SPGE biosensor was evaluated using the  $i-t$  technique, as shown in Fig. 4a. The current response of the biosensor was enhanced with the increase of glucose concentration. The rapid current response was due to the cooperation of high activity of AuNPs and the conductivity of rGO. In Fig. 4b, low concentration glucose molecules

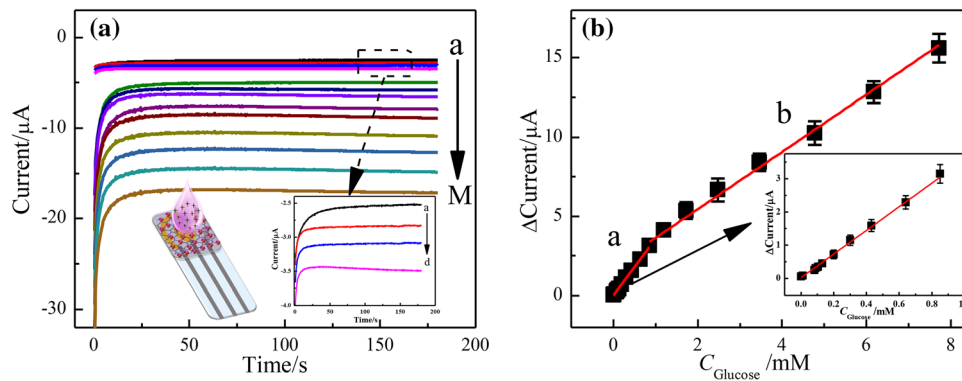


**Figure 4** (a) Amperometric response of the glucose sensor with glucose concentration of 0.00125, 0.13, 0.20, 0.30, 0.64, 0.85, 1.2, 1.72, 2.48, 3.47, 4.78, 6.17, 7.72 mM in 0.1 M PBS, pH 7.4,

−0.3 V. (b) The calibration curve of GOx-gel-rGO-Au/SPGE in different concentrations of glucose (Inset: the magnifying linear plots at low concentration of glucose).

**Table 1** Comparison of proposed work with other reported glucose biosensors

Electrode	Sensitivity (μA/mM cm <sup>2</sup> )	LOD (μM)	Linear range (mM)	References
GOx/PB/graphene	18	10	0.2–1.0	[29]
MWCNTs-PB/Carbon WE	105.9	4.95	0.5–1.0	[28]
GOx/3D-printed G-PLA electrode	3.63	15	0.5–6.3	[30]
CS/SWCNTs-GOD/PB/v-AuNWs	23.7	10	0–1.4	[31]
CS/GOD/PB/Au/Au NWs & SEBS	11.7	6	0–500	[26]
ZnO TPs/MXene/GOx	29	17	0.05–0.7	[32]
GOx/AuNPs/Pty/PB/SPCE	16.7	1.0	0.0010–1.0	[33]
CHIT(GOx)/AuLr-TiND	13.23	14.38	0.10–7.52	[34]
	3.79		7.52–40	
Ti <sub>3</sub> C <sub>2</sub> -PLL-GOx	71.42	4.2	0.004–0.02	[35]
	38.18		0.02–1.1	
Au/CNT/b2LOxS/PEI-PEGDGE/C	5.6	57	0.1–5.0	[36]
GOx-gel-rGO-Au/SPGE	53.7	1.25	0.00125–0.85	This work
	27.4		0.85–7.72	

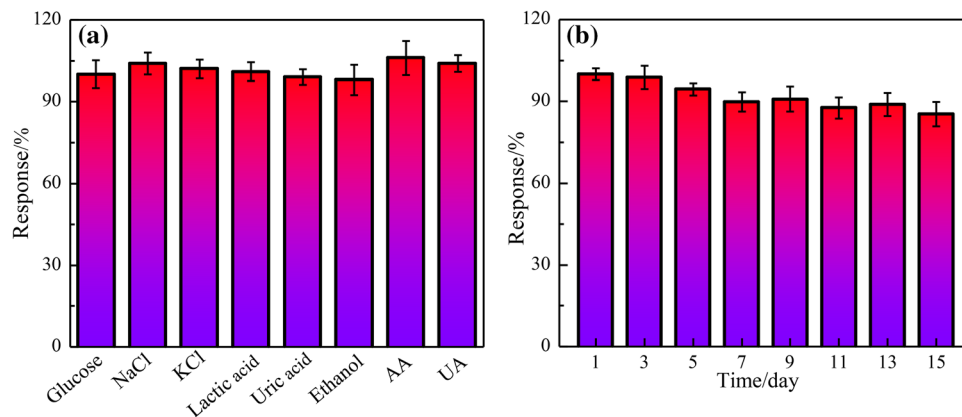
diffuse rapidly in gel, and the sensitivity of the biosensor was improved. With the increase of glucose concentration, the diffusion of glucose molecules in gel gradually flattens and tends to saturation. This indicates that there are two linear relationships between glucose concentration and current response value. The first linear segment increases from 1.25 to 850 μM with a linear regression equation of  $I_a$  (μA) = 3.555C<sub>glu</sub> (mM) + 0.024 (R<sup>2</sup> = 0.994), and the second linear segment increases from 0.85 to 7.72 mM with a linear regression equation of  $I_b$  (μA) = 1.809C<sub>glu</sub> (mM) + 1.834 (R<sup>2</sup> = 0.994). The sensitivity of the biosensor was 53.7 μA/mM cm<sup>2</sup> and 27.4 μA/mM cm<sup>2</sup>, respectively. And the limit of detection (LOD) was estimated to be 1.25 μM, which was suitable the practical requirements of sweat

glucose levels in humans (0.01–1 mM is typical glucose concentrations in human sweat) [13, 28]. Table 1 displayed a comparison between this work and the previously published glucose biosensors. The biosensor exhibited wide linear range, low detection limit and high sensitivity for glucose detection, indicating that it has a bright application prospect in flexible wearable medical detection platform.

PB: Prussian blue; MWCNTs-PB: mixture of multi-walled carbon nanotubes and Prussian blue; carbon WE: carbon working electrode; G-PLA: graphene-polylactic acid; CS: chitosan; SWCNTs: single-walled carbon nanotubes; GOD: glucose oxidase; v-Au NWs: vertically aligned Enokitake-like gold nanowires; Au NWs: gold nanowires; SEBS: styrene-ethylene-butadiene-styrene; ZnO TPs: ZnO tetrapods; GOx:



**Figure 5** (a) Electrochemical response of 0.10 mM glucose and added 0.1 mM NaCl, 0.1 mM KCl, 3 mM lactic acid, 3 mM uric acid, 3 mM ethanol and 1 mM UA, respectively. (b) Storage stability of the biosensor..



glucose oxidase; Pty: polytyramine layer; SPCE: screen-printed carbon electrodes; PLL: poly-L-lysine; CNT: carbon nanotubes; b2LOxS: DET-type engineered LOx; PEGDGE: poly(ethylene glycol) diglycidyl ether.

Selectivity plays an important role in the performance of glucose biosensor. Some interfering substances including NaCl, KCl, lactic acid, uric acid, ethanol, UA and AA were added to glucose. As shown in Fig. 5a, the GOx-gel-rGO-Au/SPGE has no obvious response to interfering substances due to the selective oxidation of GOx fixed on the surface of the working electrode, which indicates that the GOx-gel-rGO-Au/SPGE-based biosensor has excellent selectivity for glucose detection. Therefore, GOx-gel-rGO-Au/SPGE could be expected to be highly selective for glucose detection.

Good reproducibility and stability are the key parameters to evaluate the success of the biosensor in practical applications. In Fig. S4A, five flexible sensors were randomly selected from the same batch to test 1.2 mM glucose under the same experimental conditions, and the RSD of the test results was only 3.0%. In order to meet the application of wearable sensors in daily monitoring, a single sensor needs to be used multiple times. After measuring the same electrode for 5 consecutive times, the RSD of the test results shall not be greater than 5.2% (Fig. S4B). These results indicate that the prepared GOx-gel-rGO-Au/SPGE glucose biosensor possessed a good stability and reproducibility. To evaluate the storage stability of the biosensor, the as-prepared GOx-gel-rGO-Au/SPGE biosensors were sealed and stored at 4 °C. As shown in Fig. 5b, the biosensors could retain 85.3% of the initial current response after 15 days. The results indicated that the proposed biosensor has

acceptable storage stability which may meet the needs of long-distance transportation and real-time monitoring.

Since wearable sensors need to be attached to the body, their bending durability is another critical factor. The electrochemical stability of the biosensor in the bending state was obtained by testing at different bending radii and different bending times. As shown in Fig. S4C, the device based on GOx-gel-rGO-Au/SPGE still maintains stable electrochemical performance within a bending radius of 0.3–1 mm. Even the extreme condition ( $R_c = 0.3$  mm), the current response value of the biosensor remains at 81.6% of the initial value. Moreover, the flexible biosensor based on the GOx-gel-rGO-Au/SPGE retained 79.1% of their initial electrochemical after 1700 bending cycles (Fig. S4D). These good mechanical stabilities indicate that glucose biosensor based on GOx-gel-rGO-Au/SPGE has good tensile properties.

### Real sample analysis

To verify its feasibility for in practical applications, the GOx-gel-rGO-Au/SPGE biosensor was applied for determination of glucose in human sweat. Fresh sweat from two volunteers was collected as actual samples. Meanwhile, spectrophotometry method was used to evaluate the accuracy of the constructed biosensor, and the corresponding recoveries were exposed in Table 2. The determination results of electrochemical method based on GOx-gel-rGO-Au/SPGE were consistent with the spectrophotometric method, and the error was small. This manifests that the GOx-gel-rGO-Au/SPGE biosensor has stable performance and high accuracy, which could be used to determine the glucose in sweat. On the other hand, in

**Table 2** Detection results of glucose in human sweat samples

Sample No	Found (Spectrophotometry method) ( $\mu\text{M}$ )	Average found (Electrochemical method) ( $\mu\text{M}$ )	Corresponding Recovery (%)	RSD (% $n = 3$ )
1	63.72	64.67	101.5	1.8
2	89.29	88.25	98.9	2.3

order to more intuitively verify the application of the biosensor in the actual test, we directly attached the biosensor to the palm of the volunteers who had just exercised for 15 min and observed the change of the current. In Movie S1, it is clearly observed that the current of the biosensor gradually rises and stabilizes. This means that the contact between the biosensor and the skin surface was stable, and the sweat was collected through the gel and reacted with the electrode to generate electrical changes. This confirmed that it is possible that the constructed GOx-gel-rGO-Au/SPGE biosensor could be worn on the human skin surface and measure glucose in sweat in real time and online.

## Conclusions

In summary, a novel flexible wearable electrochemical biosensor was constructed for simple determination of glucose in human sweat. Compared with traditional methods, using soft gels instead of liquid electrolytes not only allows measure glucose with fewer samples, but also adapts to the variability of human movement. Under the synergistic effect of the nanocomposite catalyst of rGO-Au/SPGE and the specific selection of GOx, GOx-gel-rGO-Au/SPGE biosensor has excellent catalytic activity and anti-interference performance for glucose. The biosensor maintained stable sensing performance after 1000 bending cycles, demonstrating good bending resistance. In addition, the detection results of the biosensor in human sweat were comparable to those of commercial kits, indicating its excellent accuracy and anti-interference performance. Therefore, we believe that the combination of nanocatalysts with gel electrolyte has great potential for non-invasive and wearable health monitoring.

## Acknowledgements

This work was supported by the National Natural Science Foundation of China (Nos. 51672074, 52272106), the Natural Science Foundation of Hubei Province, China (No. 2019CFA006), and the Program for Science and Technology Innovation Team in Colleges of Hubei Province (No. T201901).

## Funding

National Natural Science Foundation of China, 52272106, Gang Chang, 51672074, Gang Chang, Natural Science Foundation of Hubei Province, 2019CFA006, Yunbin He, the Program for Science and Technology Innovation Team in Colleges of Hubei Province, T201901, Yunbin He.

## Declarations

**Conflict of interest** The authors declare that they have no known competing financial interests or personal relationships that could have appeared to influence the work reported in this paper.

**Supplementary Information:** The online version contains supplementary material available at <https://doi.org/10.1007/s10853-022-08095-7>.

## References

- [1] Lou Z, Wang L, Jiang K, Wei Z, Shen G (2020) Reviews of wearable healthcare systems: materials, devices and system integration. *Mater Sci Eng: R: Rep* 140:100523. <https://doi.org/10.1016/j.mser.2019.100523>
- [2] Yoon J, Lee SN, Shin MK, Kim HW, Choi HK, Lee T, Choi JW (2019) Flexible electrochemical glucose biosensor based on GOx/gold/MoS<sub>2</sub>/gold nanofilm on the polymer electrode.

- Biosens Bioelectron 140:111343. <https://doi.org/10.1016/j.bios.2019.111343>
- [3] Shi C, Zou Z, Lei L, Zhu Z, Zhang Z, Xiao X (2020) Heterogeneous integration of rigid, soft, and liquid materials for self-healable, recyclable, and reconfigurable wearable electronics. *Sci Adv* 6(45):eabd0202. <https://doi.org/10.1126/sciadv.abd0202>
- [4] Ling Y, An T, Yap LW, Zhu B, Gong S, Cheng W (2020) Disruptive, soft, wearable sensors. *Adv Mater* 32(18):e1904664. <https://doi.org/10.1002/adma.201904664>
- [5] Yetisen AK, Martinez-Hurtado JL, Unal B, Khademhosseini A, Butt H (2018) Wearables in medicine. *Adv Mater* 30:e1706910. <https://doi.org/10.1002/adma.201706910>
- [6] Bariya M, Nyein HYY, Javey A (2018) Wearable sweat sensors. *Nat Electron* 1(3):160–171. <https://doi.org/10.1038/s41928-018-0043-y>
- [7] Vashist SK (2012) Non-invasive glucose monitoring technology in diabetes management: a review. *Anal Chim Acta* 750:16–27. <https://doi.org/10.1016/j.aca.2012.03.043>
- [8] Scully T (2012) Diabetes in numbers. *Nature* 485(7398):S2–S3. <https://doi.org/10.1038/485s2a>
- [9] Xiong C, Zhang T, Kong W, Zhang Z, Qu H, Chen W, Wang Y, Luo L, Zheng L (2018) ZIF-67 derived porous Co<sub>3</sub>O<sub>4</sub> hollow nanopolyhedron functionalized solution-gated graphene transistors for simultaneous detection of glucose and uric acid in tears. *Biosens Bioelectron* 101:21–28. <https://doi.org/10.1016/j.bios.2017.10.004>
- [10] Zahed MA, Barman SC, Das PS, Sharifuzzaman M, Yoon HS, Yoon SH, Park JY (2020) Highly flexible and conductive poly (3, 4-ethylene dioxythiophene)-poly (styrene sulfonate) anchored 3-dimensional porous graphene network-based electrochemical biosensor for glucose and pH detection in human perspiration. *Biosens Bioelectron* 160:112220. <https://doi.org/10.1016/j.bios.2020.112220>
- [11] Gong JP, Katsuyama Y, Kurokawa T, Osada Y (2003) Double-network hydrogels with extremely high mechanical strength. *Adv Mater* 15(14):1155–1158. <https://doi.org/10.1002/adma.200304907>
- [12] Sun JY, Zhao X, Illeperuma WR, Chaudhuri O, Oh KH, Mooney DJ, Vlassak JJ, Suo Z (2012) Highly stretchable and tough hydrogels. *Nature* 489(7414):133–136. <https://doi.org/10.1038/nature11409>
- [13] Ramadoss P, Rahman MI, Perumal A, Nallaiyan R, Basha SH, Dakshanamoorthy A (2020) Non-invasive, non-enzymatic, biodegradable and flexible sweat glucose sensor and its electrochemical studies. *ChemistrySelect* 5(36):11305–11321. <https://doi.org/10.1002/slct.202002622>
- [14] Gao W, Emaminejad S, Nyein HYY, Challa S, Chen K, Peck A, Fahad HM, Ota H, Shiraki H, Kiriya D, Lien DH, Brooks GA, Davis RW, Javey A (2016) Fully integrated wearable sensor arrays for multiplexed in situ perspiration analysis. *Nature* 529(7587):509–514. <https://doi.org/10.1038/nature16521>
- [15] Park J, Sempionatto JR, Kim J, Jeong Y, Gu J, Wang J, Park I (2020) Microscale biosensor array based on flexible polymeric platform toward lab-on-a-needle: real-time multiparameter biomedical assays on curved needle surfaces. *ACS Sens* 5(5):1363–1373. <https://doi.org/10.1021/acssensors.0c00078>
- [16] Park J, Jeong Y, Kim J, Gu J, Wang J, Park I (2020) Biopsy needle integrated with multi-modal physical/chemical sensor array. *Biosens Bioelectron* 148:111822. <https://doi.org/10.1016/j.bios.2019.111822>
- [17] Sasaki M, Karikkineth BC, Nagamine K, Kaji H, Torimitsu K, Nishizawa M (2014) Highly conductive stretchable and biocompatible electrode-hydrogel hybrids for advanced tissue engineering. *Adv Healthc Mater* 3(11):1919–1927. <https://doi.org/10.1002/adhm.201400209>
- [18] Kiani A, Asempour H (2012) Hydrogel membranes based on gum tragacanth with tunable structures and properties. II. Comprehensive characterization of the swelling behavior. *J Appl Polym Sci* 126(1):E478–E485. <https://doi.org/10.1002/app.36782>
- [19] Zhang Z, Fu H, Li Z, Huang J, Xu Z, Lai Y, Qian X, Zhang S (2022) Hydrogel materials for sustainable water resources harvesting & treatment: synthesis, mechanism and applications. *Chem Eng J* 439:135756. <https://doi.org/10.1016/j.cej.2022.135756>
- [20] Yan C, Kramer PL, Yuan R, Fayer MD (2018) Water dynamics in polyacrylamide hydrogels. *J Am Chem Soc* 140(30):9466–9477. <https://doi.org/10.1021/jacs.8b03547>
- [21] Zhou Y, Ma M, He H, Cai Z, Gao N, He C, Chang G, Wang X, He Y (2019) Highly sensitive nitrite sensor based on AuNPs/RGO nanocomposites modified graphene electrochemical transistors. *Biosens Bioelectron* 146:111751. <https://doi.org/10.1016/j.bios.2019.111751>
- [22] Tao T, Zhou Y, Ma M, He H, Gao N, Cai Z, Chang G, He Y (2021) Novel graphene electrochemical transistor with ZrO<sub>2</sub>/rGO nanocomposites functionalized gate electrode for ultrasensitive recognition of methyl parathion. *Sens Actuators B: Chem* 328:128936. <https://doi.org/10.1016/j.snb.2020.128936>
- [23] Xu D, Zhu C, Meng X, Chen Z, Li Y, Zhang D, Zhu S (2018) Design and fabrication of Ag-CuO nanoparticles on reduced graphene oxide for nonenzymatic detection of glucose. *Sens Actuators, B Chem* 265:435–442. <https://doi.org/10.1016/j.snb.2018.03.086>
- [24] Liu X, Zhang W, Lin Z, Meng Z, Shi C, Xu Z, Yang L, Liu X (2021) Coupling of silk fibroin nanofibrils enzymatic membrane with ultra-thin PtNPs/graphene film to acquire

- long and stable on-skin sweat glucose and lactate sensing small. *Methods* 5(3):2000926. <https://doi.org/10.1002/smt.202000926>
- [25] Gao N, He C, Ma M, Cai Z, Zhou Y, Chang G, Wang X, He Y (2019) Electrochemical co-deposition synthesis of Au-ZrO<sub>2</sub>-graphene nanocomposite for a nonenzymatic methyl parathion sensor. *Anal Chim Acta* 1072:25–34. <https://doi.org/10.1016/j.aca.2019.04.043>
- [26] Zhao Y, Zhai Q, Dong D, An T, Gong S, Shi Q, Cheng W (2019) Highly stretchable and strain-insensitive fiber-based wearable electrochemical biosensor to monitor glucose in the sweat. *Anal Chem* 91(10):6569–6576. <https://doi.org/10.1021/acs.analchem.9b00152>
- [27] Bai Y, Chen B, Xiang F, Zhou J, Wang H, Suo Z (2014) Transparent hydrogel with enhanced water retention capacity by introducing highly hydratable salt. *Appl Phys Lett* 105(15):151903. <https://doi.org/10.1063/1.4898189>
- [28] Zheng L, Liu Y, Zhang C (2021) A sample-to-answer, wearable cloth-based electrochemical sensor (WCECS) for point-of-care detection of glucose in sweat. *Sens Actuators B: Chem* 343:130131. <https://doi.org/10.1016/j.snb.2021.130131>
- [29] Naik AR, Zhou Y, Dey AA, Arellano DLG, Okoroanyanwu U, Secor EB, Hersam MC, Morse J, RothsteinCarter JPKR (2022) Printed microfluidic sweat sensing platform for cortisol and glucose detection. *Lab Chip* 22(1):156–169. <https://doi.org/10.1039/d1lc00633a>
- [30] Cardoso RM, Silva PRL, Lima AP, Rocha DP, Oliveira TC, do Prado TM, Fava EL, Fatibello-Filho O, Richter EM, Muñoz RAA (2020) 3D-Printed graphene/polylactic acid electrode for bioanalysis: biosensing of glucose and simultaneous determination of uric acid and nitrite in biological fluids. *Sens Actuators B: Chem* 307:127621. <https://doi.org/10.1016/j.snb.2019.127621>
- [31] Zhai Q, Gong S, Wang Y, Lyu Q, Liu Y, Ling Y, Wang J, Simon GP, Cheng W (2019) Enokitake mushroom-like standing gold nanowires toward wearable noninvasive bimodal glucose and strain sensing. *ACS Appl Mater Interfaces* 11(10):9724–9729. <https://doi.org/10.1021/acsami.8b19383>
- [32] Myndrul V, Coy E, Babayevska N, Zahorodna V, Balitskiy V, Baginskiy I, Gogotsi O, Bechelany M, Giardi MT, Iat-sunskyi I (2022) MXene nanoflakes decorating ZnO tetrapods for enhanced performance of skin-attachable stretchable enzymatic electrochemical glucose sensor. *Biosens Bioelectron* 207:114141. <https://doi.org/10.1016/j.bios.2022.114141>
- [33] Khumngern S, Jirakunakorn R, Thavarungkul P, Kanatharana P, Numnuam A (2021) A highly sensitive flow injection amperometric glucose biosensor using a gold nanoparticles/polytyramine/Prussian blue modified screen-printed carbon electrode. *Bioelectrochemistry* 138:107718. <https://doi.org/10.1016/j.bioelechem.2020.107718>
- [34] Lipińska W, Siuzdak K, Karczewski J, Dołęga A, Grochowska K (2021) Electrochemical glucose sensor based on the glucose oxidase entrapped in chitosan immobilized onto laser-processed Au-Ti electrode. *Sens Actuators B: Chem* 330:129409. <https://doi.org/10.1016/j.snb.2020.129409>
- [35] Wu M, Zhang Q, Fang Y, Deng C, Zhou F, Zhang Y, Wang X, Tang Y, Wang Y (2021) Polylysine-modified MXene nanosheets with highly loaded glucose oxidase as cascade nanoreactor for glucose decomposition and electrochemical sensing. *J Colloid Interface Sci* 586:20–29. <https://doi.org/10.1016/j.jcis.2020.10.065>
- [36] Li M, Wang L, Liu R, Li J, Zhang Q, Shi G, Li Y, Hou C, Wang H (2021) A highly integrated sensing paper for wearable electrochemical sweat analysis. *Biosens Bioelectron* 174:112828. <https://doi.org/10.1016/j.bios.2020.112828>

**Publisher's Note** Springer Nature remains neutral with regard to jurisdictional claims in published maps and institutional affiliations.

Springer Nature or its licensor (e.g. a society or other partner) holds exclusive rights to this article under a publishing agreement with the author(s) or other rightsholder(s); author self-archiving of the accepted manuscript version of this article is solely governed by the terms of such publishing agreement and applicable law.